

# Computer Simulation of a Single-Torch System and the Interaction of the Several Capillary Torches

Victor V. Kuzenov  
N.L. Dukhov All-Russian Research  
Institute of Automatics (State  
Corporation «ROSATOM» company)  
Moscow, Russia  
vik.kuzenov@gmail.com

Sergei V. Ryzhkov  
Thermal Physics Department  
Bauman Moscow State Technical  
University  
Moscow, Russia  
svryzhkov@bmstu.ru

Konstantin V. Polyakov  
Thermal Physics Department  
Bauman Moscow State Technical  
University  
Moscow, Russia  
konstantin.vl.p@mail.ru

**Abstract**—A capillary discharge with an evaporating wall, namely system of pulsed plasma jets is considered. The structure of an underexpanded supersonic jet that expires from the plasma channel of the capillary discharge with an evaporating wall is investigated. The turbulent viscosity and thermal conductivity coefficients are calculated using the equations of the Coakley model. Numerical simulation is performed and spatial distributions of plasma pressure, and temperature for an array of three pulsed plasma jets at different moments of time are obtained.

**Keywords**—capillary discharge, MHD and plasma, numerical simulation, plasma jets, pulsed system

## I. INTRODUCTION

Pulsed capillary discharge is one of the relatively simple methods of plasma formation. It is known that this type of discharge is characterized by a long, sufficiently stable in the atmosphere plasma structure of the pulsed jet [1-8]. The flow pattern can be described as follows. After the breakdown stage, a plasma formation is formed near the capillary wall, serving as a source of thermal broadband radiation, which, acting on the wall, causes heating of the surface layer of the capillary wall and later its evaporation. It is known that evaporation begins at the end of the capillary (from the time  $t = 1.3 \mu\text{s}$ , and at  $t = 1.75 \mu\text{s}$ , evaporation reaches the central zone of the surface, while the surface temperature is  $T = 0.5 \text{ eV}$ ), and further the wave evaporation spreads to the center of the tube. The current flow in the vapor of the wall material is accompanied by their heating up to the plasma state (with a corresponding increase in pressure and temperature) and flow (as a rule, with sound velocities) through the capillary outlet into the surrounding gas. At the same time, in the torch of a pulsed capillary discharge a flow structure close to the structure appears, which is characteristic of the initial section of the flow in a stationary supersonic plasma jet flowing into an air atmosphere. If the pressure at the cross-section of the nozzle  $P_a$  divided by the pressure in the unperturbed environment  $P_\infty$ , then a determining complex is formed, called the degree of incorrectness  $n = P_a/P_\infty$ . It is known that if the degree of incorrectness  $n \approx 1$  is close to unity, then the capillary discharge torch consists of several cycles of the periodic wave structure, called «barrel». At values of  $n \gg 1$ , only one «barrel» is formed. A capillary discharge with an evaporating wall is considered below.

## II. MATHEMATICAL MODEL FOR COMPUTER SIMULATION OF THE MAIN PARAMETERS OF THE INTERACTING CAPILLARY TORCHES

The mathematical model of the processes occurring in the plasma of a capillary discharge is based on the multicomponent radiation equations of Reynolds. To solve the system of equations by a finite difference method, the coordinate transformation is introduced in the following form:  $r = r(\xi, \eta, \zeta)$ ,  $z = z(\xi, \eta, \zeta)$ ,  $\varphi = \varphi(\xi, \eta, \zeta)$ . Plasma dynamic processes in capillary discharge plasmas can be determined using a system of equations for viscous one-temperature radiation plasma dynamics.

Thus, the system of RMHD equations in capillary discharge channel has the following form:

$$\begin{aligned} \frac{\partial \rho c_i}{\partial t} + \text{Div}(\rho c_i \vec{V}) &= -\alpha \frac{\rho c_i u}{r} + \text{Div}(\rho D_i \nabla c_i) + \left( \frac{\partial \rho c_i}{\partial t} \right)_x \quad (1) \\ \frac{\partial \rho}{\partial t} + \text{Div}(\rho \vec{V}) &= -\alpha \frac{\rho u}{r}, \\ \frac{\partial \rho u}{\partial t} + \text{Div}(\rho u \vec{V}) &= -\xi_r \frac{\partial P}{\partial \xi} - \eta_r \frac{\partial P}{\partial \eta} - \alpha \frac{\rho u^2}{r} + \frac{S_r}{\text{Re}}, \\ \frac{\partial \rho v}{\partial t} + \text{Div}(\rho v \vec{V}) &= -\xi_z \frac{\partial P}{\partial \xi} - \eta_z \frac{\partial P}{\partial \eta} - \alpha \frac{\rho v}{r} + \frac{S_z}{\text{Re}}, \\ \frac{\partial \rho e}{\partial t} + \text{Div}(\rho e \vec{V} + \sum \bar{q}_i) &= -\frac{P}{J} \text{Div}(\vec{V}) - \alpha \frac{Pu}{r} - \alpha \frac{\rho e u}{r} + \frac{S_e}{\text{Re}} + D_x, \\ S_e &= \mu_\Sigma D + \frac{\gamma}{\text{Pr}} \text{div}(\lambda_\Sigma \text{grad} T), \\ D_x &= \sum_i h_i \frac{t_*}{e_*} \text{Div}(\rho D_i \nabla c_i), \\ \text{Div}(\ ) &= \frac{1}{J} \frac{\partial (J)}{\partial \xi} + \frac{1}{J} \frac{\partial (J)}{\partial \eta}, \end{aligned}$$

where  $r$  is the radial coordinate,  $\rho$  is the plasma density,  $u$  is the velocity along the coordinate,  $v$  is the velocity perpendicular the coordinate,  $P = P(\rho, e)$  is the static pressure,  $e$  is the specific internal energy of plasma,  $S_r$ ,  $S_z$  are the forces [9-10], arising in the torch of the capillary discharge due to the

This work was supported by the Ministry of Education and Science of the Russian Federation (Project No 13.5240.2017/8.9).

presence in it of viscous friction forces,  $S_e$  is the volumetric (specific) energy release,  $Re$  is the Reynolds number,  $Pr$  is the Prandtl number,  $u(r,z,t), v(r,z,t)$  is the projection of the velocity vector  $\vec{V}(r,z,t)$  on the axis  $R$  and  $Z$ ,  $J = \partial(r,z)/\partial(\xi,\eta)$  is the Jacobian of transition from a cylindrical coordinate system  $r,z$  to a curvilinear coordinate system  $\xi,\eta$ ,  $V_\xi = \xi_r u + \xi_z v$ ,  $V_\eta = \eta_r u + \eta_z v$  are the contravariant components of the velocity vector  $\vec{V}(r,z,t)$  in the curvilinear coordinate system  $\xi,\eta$ ,  $\rho, P$  are the density and pressure of plasma,  $\sum_i q_{i\xi}, \sum_i q_{i\eta}$  are the projections of the vector of the energy flux density  $\vec{q}$  on the axis of the curvilinear coordinate system  $\xi$  and  $\eta$ ,  $\alpha = 0$  corresponds to the flat geometry,  $\alpha = 1$  corresponds to the one-dimensional cylindrical geometry.

For determination the plasma density  $\rho_g \in [0,1]$  of the ablating vapor of the capillary-wall material an additional equation of continuity is introduced into the system above the above equations:  $\frac{\partial \rho_g}{\partial t} + \vec{V} \nabla \rho_g = 0$ .

The transfer of broadband radiation is considered using a multigroup diffusion approximation, the equations of which look as follows:

$$\frac{1}{J} \frac{\partial (J q_{i\xi})}{\partial \xi} + \frac{1}{J} \frac{\partial (J q_{i\eta})}{\partial \eta} + \chi_i c U_i = 4 \chi_i \sigma_i T^4, \quad (2)$$

$$\frac{c}{3} \frac{\partial U_i}{\partial \xi} + \chi_i q_{i\xi} = 0, \quad \frac{c}{3} \frac{\partial U_i}{\partial \eta} + \chi_i q_{i\eta} = 0,$$

where  $U_i(y,z,t)$  is the bulk density of broadband radiation for  $i$ -th spectral group,  $\chi_i$  is the absorption coefficient.

Calculation of the optical parameters  $\chi_i(T, \rho)$  included in this system of equations for working media was carried out using the ASTEROID computer system [11]. When calculating the optical characteristics, the all spectrum was divided into 7 groups with interval boundaries [0.1-3.14-5.98-6.52-7.95-9.96-18.6-200] eV, where the environmental medium is air. The turbulent coefficients of viscosity  $\mu_\Sigma$  and thermal conductivity  $\lambda_\Sigma$  are calculated using equations  $q-\omega$  ( $q$  is a pseudo velocity and  $\omega$  is a pseudo vortex) of the Coakley differential model in the curvilinear coordinates  $\xi,\eta$  [12].

The solution of two-dimensional non-stationary equations of viscous one-temperature radiation plasma dynamics written in a vector semi-divergent form in a curvilinear coordinates and reproduced above:

$$\frac{\partial \vec{U}}{\partial t} + \frac{\partial \vec{F}}{\partial \xi} + \frac{\partial \vec{G}}{\partial \eta} + \vec{S} = \frac{1}{Re} \left[ \frac{\partial \vec{F}_v}{\partial \xi} + \frac{\partial \vec{G}_v}{\partial \eta} + \vec{S}_v \right] \quad (3)$$

is written using the splitting method for physical processes and directions. The type of the vectors entering into the given system of equations is indicated in [10].

At the first fractional time step  $t \in [t, t + \Delta t/3]$  the nonlinear quasimonotone compact polynomial finite-difference scheme of high order of accuracy, developed in [9-10], is used:

$$\frac{\partial \vec{U}_{i,j}}{\partial t} + \frac{\vec{F}_{i+1/2,j} - \vec{F}_{i-1/2,j}}{\Delta \xi} + \frac{\vec{G}_{i,j+1/2} - \vec{G}_{i,j-1/2}}{\Delta \eta} + \vec{S}_{i,j} = 0. \quad (4)$$

At second time step  $t \in [t + \Delta t/3, t + 2\Delta t/3]$  the ‘‘parabolic’’ (‘‘viscous’’) part of the system of equations is solved by an explicit method with use of boundary conditions of ‘‘sticking’’. The first and second derivatives in space, included in the system of equations for the second time fractional step, were obtained by means of a quasi-monotonic compact polynomial finite difference scheme of high order [9-10].

The third fractional time step  $t \in [t + 2\Delta t/3, t + \Delta t]$  concludes the computation of ‘‘hard’’ part of the system of equations  $q-\omega$  of the Coakley model using an implicit Rosenbrock method. The time step  $\Delta t$  required for integrating the above differential scheme is found using the Courant–Friedrichs–Lewy condition. A modified alternate-triangular method is applied when solving the radiation transfer equations, using a three-layer iteration scheme where the iteration ‘‘time’’ step is found by the conjugate direction method [13].

Parameters of the plasma flowing from the capillary discharge channel to the low pressure area, when performing gas dynamic calculations, were determined on the basis of the approximate mathematical model. It was assumed that all electrical energy stored in capacitive storage is transformed into thermal energy of the plasma, which expires with the speed of sound through the capillary discharge section.

### III. RESULTS FOR PULSED PLASMA JETS

The calculating area in the coordinate system  $r,z$  and  $\xi,\eta$  is a rectangle. The calculated area in the coordinate system is a rectangle. In the lower part of the rectangle, a capillary discharge is located perpendicular to the surface, which is the source of the erosive plasma torch of the capillary discharge. From above it was bounded by a straight line on which set the ‘‘non-perturbing’’ conditions on the flow emerging from the computational domain:  $\partial^2 \vec{f} / \partial x_n^2 = 0$ ,  $\vec{f} = \{\rho, u, v, e\}$  and  $x_n$  is the coordinate normal to the boundary surface. On the right side, the integration region is limited by the symmetry axis, on which the corresponding symmetry conditions for the plasma flow are given. On the left side there is a surface located at a

sufficient distance from the axis of symmetry, so a given set of boundary conditions must be provided corresponding to the conditions at infinity in the unperturbed gaseous medium.

The capillary discharge consists of an interelectrode insert with an axial hole, which is the working channel of the discharge (the diameter of the capillary discharge is 1 mm, the length is 5 mm). A plasma flow is injected through the walls of the capillary with parameters taken from [14]:  $T = 35$  kK,  $V = 450$  m/s,  $P = 41$  MPa,  $\gamma = 1.2$ . When carrying out numerical calculations, these values are redefined (by calculation, from the condition of the sonic flow in the output section of the capillary discharge) in the output section of the discharge. The values  $q-\omega$  were found from the condition that the degree of turbulence in the flow flowing into the calculated region is 5%.

The peculiarity of the dynamics inside the torch discharge plasma is the flow in the region of the triple shock wave configuration. Here at the Mach disk (in later times), formed the vortex trace. Here at the Mach disk (in later times), formed the vortex trace. This trail is associated with the fact that the velocity head of a stream which has undergone 2-stage compression, many times more than pressure head for the central leap [15].

Experimental and theoretical [15-19] studies of a pulsed jet flowing through a section of a single capillary discharge show that toroidal long-lived vortex structures are formed in the region of mixing of the jet and the surrounding gaseous medium. One of the main and important properties of the toroidal vortex (TV) is that it passes in an unbounded medium before its decay, large distances in comparison with a cloud (plasma, gas, liquid) of the same size as the vortex. So, the distance TV traveled prior to its dissolution may reach a value  $z_{\max} \approx (60 \div 150)R_0$  depending on their initial parameters ( $R_0$  is initial radius of the TV).

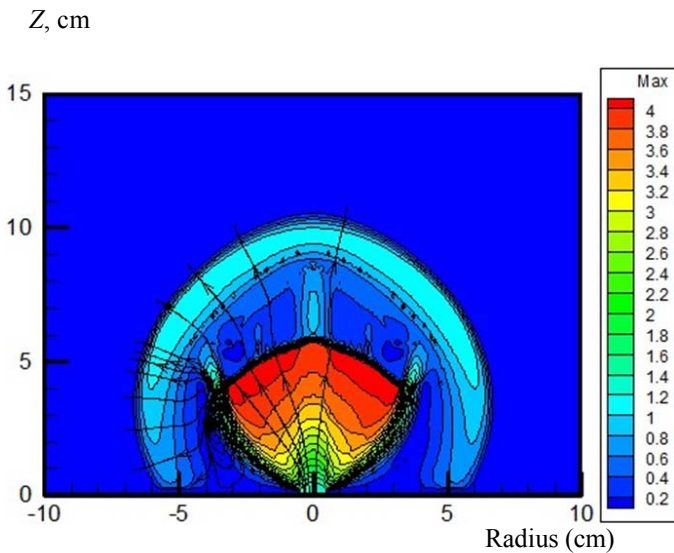


Fig. 1. The Mach number distribution over the jet axis for a single jet formed by capillary discharge with an evaporating wall at time  $t = 58.2 \mu\text{s}$ .

Figs. 1-4 show two-dimensional spatial distributions of Mach number, pressure, and longitudinal velocity at time  $t = 58.2 \mu\text{s}$  for  $W_0 = 2.7$  kJ,  $d = 10$  mm,  $P_\infty = 1$  atm for a plasma jet generated in atmospheric-pressure pulsed capillary discharge.

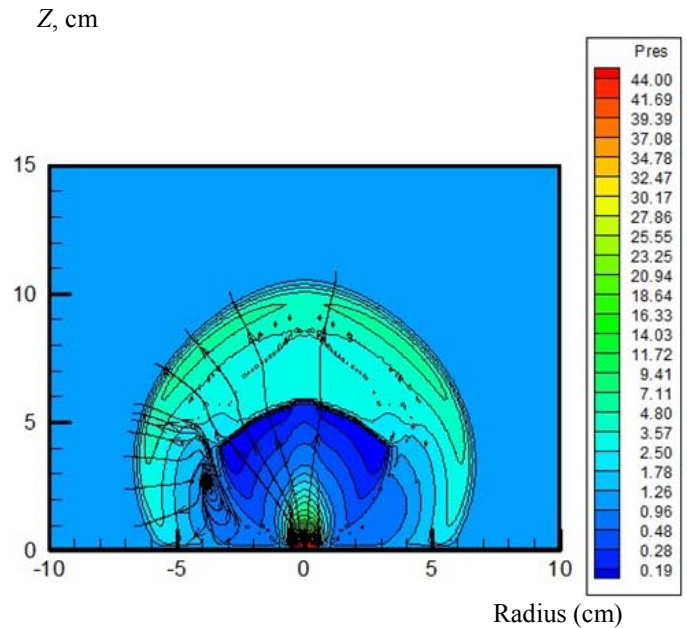


Fig. 2. The plasma pressure distribution in the plasma jet at time  $t = 58.2 \mu\text{s}$ .

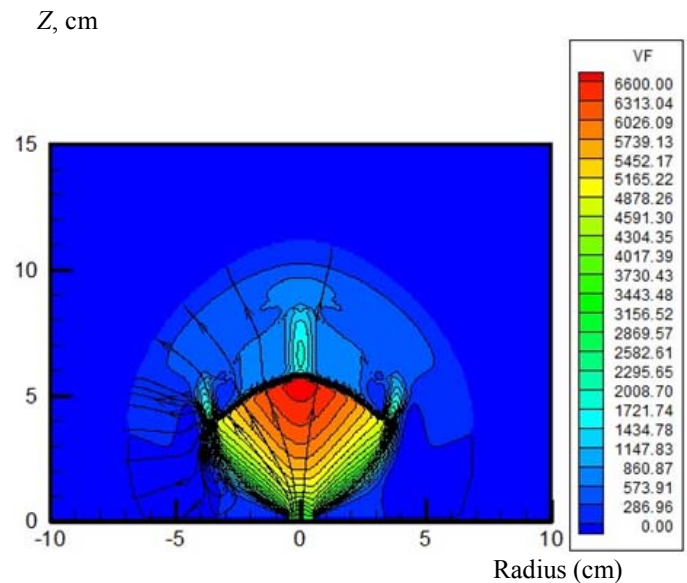


Fig. 3. The spatial distribution of the longitudinal velocity (the projection on the Z axis) in the capillary discharge jet at time  $t = 58.2 \mu\text{s}$ .

As can be seen from the spatial distributions shown in Figs. 1 – 3, also the origin and development of primary toroidal vortex structure occurs at the initial stage (at time  $t = 58.2 \mu\text{s}$ ).

Free shear flows (jets, traces, mixing layers, shear layers) are often found in technical devices. One of the important

features of shear flows is instability (one of the main causes of hydrodynamic instability is the shear of the velocity (in this case, longitudinal flow), that is, the presence of inflection points in its profile), which leads to the formation of large-scale vortex structures. That is, in the presence of tangential discontinuity, the motion of a pulsed jet is exponentially unstable with respect to any wave-like perturbation, the growth rate of which depends on the wave number  $k = 2\pi / \lambda$  ( $\lambda$  is the wavelength) and is equal to  $\gamma = kU$  ( $U$  is the magnitude of the velocity shift). We note that the elimination of the velocity discontinuity (which is observed for  $t \geq 144 \mu\text{s}$ ) leads to the stabilization of the flow with respect to small-scale perturbations.

A numerical study of the interaction of a system of pulsed jets emanating from a capillary discharge may be of particular interest to the magneto-inertial fusion, plasma technology and aerodynamics. Figs. 4 - 7 show two-dimensional (2D) spatial distributions of temperature  $T$ , K and pressure  $P$ , atm for plasma jets, created by an ablative capillary discharge.

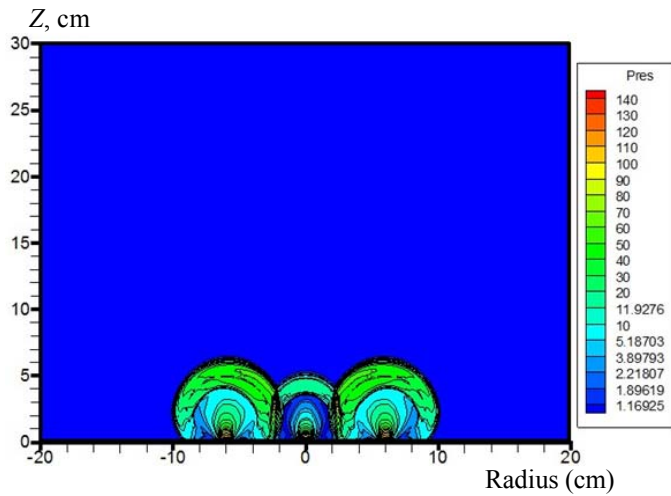


Fig. 4. Spatial distribution of the plasma density  $P$ , atm for the triple pulsed plasma jets, formed by capillary discharge with an evaporating wall at time  $t = 18.5 \mu\text{s}$ .

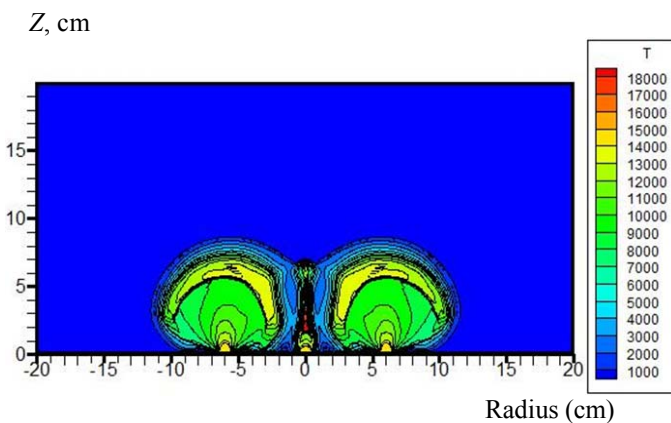


Fig. 5. The two-dimensional spatial distribution of plasma temperature  $T$ , K for an array of three pulsed plasma jets, generated by capillary discharge at time  $t = 29.8 \mu\text{s}$ .

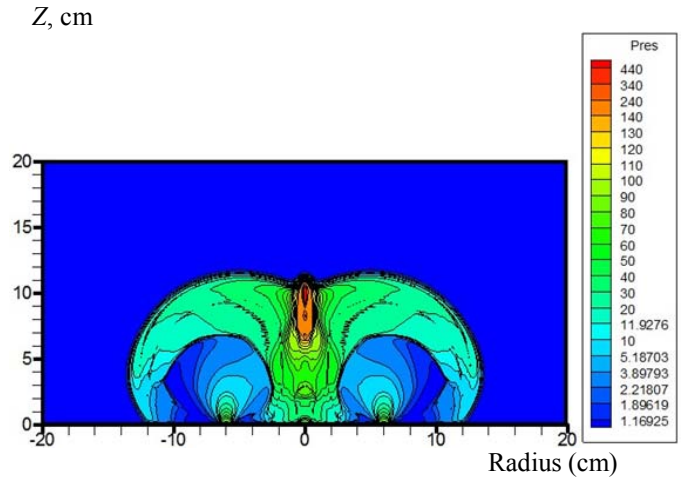


Fig. 6. The two-dimensional spatial distribution of plasma pressure  $P$ , atm for the triple pulsed plasma jets at time  $t = 41.6 \mu\text{s}$ .

The spatial distributions shown on Fig.4 - Fig.5 correspond to the beginning of the interaction of the peripheral parts of the pulsed plasma jets that flow from the capillary discharge system. First of all, this interaction affects external shock waves separating the plasma of each capillary discharge from the gaseous medium (air).

In this area there is a collision of two shock waves collide with a noticeable increase in the values of the gas-dynamical parameters in the zone of interaction (pressure and density increase approximately twice). In this case, outside the interaction zone (at a given instant in time), the thermodynamic parameters correspond to the values in the torch of a single capillary discharge.

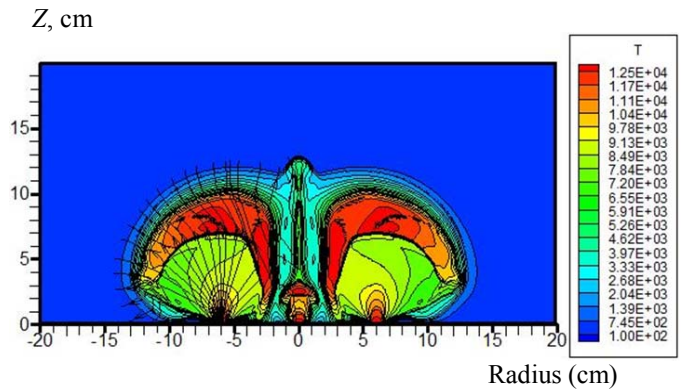


Fig. 7. Spatial distribution of the plasma temperature  $T$ , K for an array of three pulsed plasma jets, created by a capillary discharge with an evaporating wall at  $t = 48.6 \mu\text{s}$ .

Figs. 6 - 7 show that by the time  $t = 41.6 \mu\text{s}$  the plasma torch is a single whole with noticeable structural features. Thus, for example, the interaction of the capillary discharges leads to

an increase in pressure near the axis of the system ( $r \approx 0.5$  cm), relative to the environment, ( $\approx 160$  times) and density  $\approx 10$  times). The pressure in this region “locks” (at this time) the expiration of the plasma jet from capillary discharge channel, which is located on the axis of the system. In the subsequent moments of time in this area a narrowly-directed jet is formed, which has an increased axial speed of movement of the torch, in comparison with peripheral capillary discharge. It is also seen that at this stage of development of the combined plasma torch, the toroidal vortex structure has not been observed yet. It should be noted that all observed phenomena require further detailed and comprehensive study. It has been experimentally established in [14] that the position of the central shock is not sensitive to the adiabatic exponent of the working gas, condensation, nozzle edge configuration and absolute pressure, but is determined only by the degree of expansion in accordance with formula:  $p_0/p_\infty = 2,4(X_M/D)^2$ , where  $X_M$  is the distance from the capillary outlet to the Mach disk (this formula gives the value  $X_M = 2.88$  cm for  $W = 2.7$  kJ. In the calculations  $X_M = 3.1$  cm),  $D$  is the capillary diameter.

#### IV. CONCLUSION

The gas dynamics of the atmospheric pressure jet system was studied with use of a computer simulation. The interaction of three pulsed jets, created by a capillary discharge with evaporating wall is considered. The mathematical model of the system of the pulsed plasma jets flowing out into the low pressure area based on plasma dynamics written in arbitrary curvilinear coordinates is developed. The radiation and gas dynamic processes occurring in the capillary discharge system that expire into the space are numerically investigated. High-order compact finite differences are applied and gas dynamic calculations are performed. A two-dimensional radiation magnetogasdynamics code is used to investigate the characteristics of capillary discharge channel for one and three jets. All the main gas-dynamic and radiative parameters of the capillary discharge system have been calculated.

#### REFERENCES

[1] N. N. Ogurtsova, I. V. Podmoshenskii and V. M. Shelemina, “Influence of the evaporation rate of the wall material on the properties of a capillary discharge plasma,” *High Temperature*, vol. 12, pp. 5–8, 1974.

[2] N. S. Kuznetsova, A. S. Yudin and N. V. Voitenko, “Characteristics of capillary discharge channel and its effect on concrete splitting-off by electro-blasting method,” *Journal of Physics: Conference Series*, vol. 830, pp. 012043, 2017.

[3] V. V. Kuzenov, S. V. Ryzhkov and P. A. Frolko, “Numerical simulation of the coaxial magneto-plasma accelerator and non-

axisymmetric radio frequency discharge,” *J. Phys.: Conf. Ser.*, vol. 830, pp. 012049, 2017.

[4] Y. V. Kratova, T. A. Khmel’ and A. V. Fedorov, “Axisymmetric expanding heterogeneous detonation in gas suspensions of aluminum particles,” *Combustion, Explosion and Shock Waves*, vol. 52, pp. 74–84, 2016.

[5] A. Sivkov, Y. Shanenkova, A. Saigash and I. Shanenkov, “High-speed thermal plasma deposition of copper coating on aluminum surface with strong substrate adhesion and low transient resistivity,” *Surface and Coatings Technology*, vol. 292, pp. 63–67, 2016.

[6] V. V. Kuzenov and S. V. Ryzhkov, “Evaluation of hydrodynamic instabilities in inertial confinement fusion target in a magnetic field,” *Problems of Atomic Science and Technology*, vol. 4 (86), pp. 103–107, 2013.

[7] V. V. Kuzenov, T. N. Polozova and S. V. Ryzhkov, “Numerical simulation of pulsed plasma thruster with a preionization helicon discharge,” *Problems of Atomic Science and Technology*, vol. 4 (98), pp. 49–52, 2015.

[8] A. Ya. Ender, V. I. Kuznetsov and I. N. Kolyshkin, “Regimes of plasma jet outflow of capillary discharge with evaporating walls,” *Tech. Phys.*, vol. 60, pp. 1720–1724, 2015.

[9] V. V. Kuzenov and S. V. Ryzhkov, “Numerical simulation of the effect of laser radiation on matter in an external magnetic field,” *J. Phys.: Conf. Ser.*, vol. 830, pp. 012124, 2017.

[10] S. V. Ryzhkov, “Current status, problems and prospects of thermonuclear facilities based on the magneto-inertial confinement of hot plasma,” *Bulletin of the Russian Academy of Sciences. Physics*, vol. 78, pp. 456–461, 2014.

[11] S. T. Surzhikov, “Computing system for solving radiative gasdynamic problems of entry and re-entry space vehicles,” *Proc. of 1st Int. Workshop on Radiation of High Temperature Gases in Atmospheric Entry*, vol. ESA-533, pp. 111–118, 2003.

[12] T. J. Coakley, “Turbulence modeling methods for the compressible Navier-Stokes equations,” *AIAA 83-1693*, 1983.

[13] V. I. Mazhukin, D. A. Malaphei, P. P. Matus and A. A. Samarskii, “Difference schemes on irregular grids for equations of mathematical physics with variable coefficients,” *Comp. Math. Math. Phys.*, vol. 41, pp. 379–391, 2001.

[14] I. V. Sharikov and S. T. Surzhikov, “Experimental study of unsteady supersonic underexpanded ablative plasma jet dynamic,” *AIAA 2005-4930*, pp. 1–11, 2005.

[15] V. G. Dulov and G. A. Lukyanov, *Gasdynamics of the Outflow Processes*, Moscow: Nauka, 1984.

[16] V. V. Kuzenov and S. V. Ryzhkov, “Approximate method for calculating convective heat flux on the surface of bodies of simple geometric shapes,” *J. Phys.: Conf. Ser.*, vol. 815, pp. 012024, 2017.

[17] V. V. Kuzenov and S. V. Ryzhkov, “Numerical modeling of laser target compression in an external magnetic field,” *Mathematical Models and Computer Simulations*, vol. 10, pp. 255–264, 2018.

[18] V. V. Kuzenov and S. V. Ryzhkov, “Developing a procedure for calculating physical processes in combined schemes of plasma magneto-inertial confinement,” *Bulletin of the Russian Academy of Sciences. Physics*, vol. 80, pp. 598–602, 2016.

[19] V. V. Kuzenov, S. V. Ryzhkov, Gavrilova A. Yu. and Skorokhod E. P. “Computer simulation of plasmadynamic processes in capillary discharges,” *High Temperature Material Processes*, vol. 18, pp. 119–130, 2014.